Transferrin's Mechanism of Interaction with Receptor 1

Miryana Hémadi, Philippe H. Kahn, Geneviève Miquel, and Jean-Michel El Hage Chahine*

ITODYS-Interfaces, Traitements, Organisation et Dynamique des Systèmes, Université Paris 7-CNRS UMR 7086, 1 rue Guy de la Brosse, 75005 Paris, France

Received June 5, 2003; Revised Manuscript Received November 21, 2003

ABSTRACT: The kinetics and thermodynamics of the interactions of transferrin receptor 1 with holotransferrin and apotransferrin in neutral and mildly acidic media are investigated at 37 °C in the presence of CHAPS micelles. Receptor 1 interacts with CHAPS in a very fast kinetic step (<1 μs). This is followed in neutral media by the interaction with holotransferrin which occurs in two steps after receptor deprotonation, with a proton dissociation constant (K_{1a}) of 10.0 ± 1.5 nM. The first step is detected by the T-jump technique and is associated with a molecular interaction between the receptor and holotransferrin. It occurs with a first-order rate constant (k_{-1}) of (1.6 ± 0.2) × 10^4 s^{-1}, a second-order rate constant (k_1) of (3.20 ± 0.2) × 10^{10} M^{-1} s^{-1}, and a dissociation constant (K_1) of 0.50 ± 0.07 μM. This step is followed by a slow change in the conformation with a relaxation time (τ_2) of 3400 ± 400 s and an equilibrium constant (K_2) of (4.6 ± 1.0) × 10^{-3} with an overall affinity of the receptor for holotransferrin [$(K_1')^{-1}$] of (4.35 ± 0.60) × 10^8 M^{-1}. Apotransferrin does not interact with receptor 1 in neutral media, between pH 4.9 and 6, it interacts with the receptor in two steps after a receptor deprotonation (K_{2a} = 2.30 ± 0.3 μM). The first step occurs in the range of 1000−3000 s. It is ascribed to a slow change in the conformation which rate-controls a fast interaction between apotransferrin and receptor 1 with an overall affinity constant [$(K_3)^{-1}$] of (2.80 ± 0.30) × 10^7 M^{-1}. These results imply that receptor 1 probably exists in at least two forms, the neutral species which interacts with holotransferrin and not with apotransferrin and the acidic species which interacts with apotransferrin. At first, the interaction of the neutral receptor with holotransferrin is extremely fast. It is followed by the slow change in conformation, which leads to an important stabilization of the thermodynamic structure. In the acidic media of the endosome, the interaction of apotransferrin with the acidic receptor is sufficiently strong and rate-controlled by a very slow change in conformation which allows recycling back to the plasma membrane.

Transferrins are considered the essential iron transport system in vertebrates and invertebrates (*1*). Most of the transferrins and mainly human serum transferrin (ST)[1] consist of a single polypeptide chain of ∼700 amino acids organized in two lobes (C and N). Each lobe contains an iron binding cleft in which iron is coordinated to four protein ligands and a synergistic carbonate anion (*2*, *3*). In a recent series of articles, we established the mechanism of iron uptake and release by the three major transferrins: ST, lactoferrin, and ovotransferrin (*4*−*7*).

In mammals, ST solubilizes iron(III) in neutral biological media. When it becomes iron-loaded on the C-site only or on both sites (holo-ST), it is recognized by transferrin receptor 1 (TFR) and to a much lesser extent by transferrin receptor 2 (*1*). The iron-loaded ST−TFR adduct that is formed is internalized in the cytoplasm by receptor-mediated endocytosis. Upon acidification of the endosome (pH ∼5.5), the iron-loaded ST−TFR adduct loses its load of iron and is recycled back to the cell surface where TFR has no affinity for iron-free ST (apo-ST) (*8*). Therefore, iron-loaded ST in its interaction with TFR constitutes the system for transport of iron from the blood stream to the cytosol (*1*, *8*, *9*).

Complete TFR was isolated from human placenta and identified in the 1980s (*10*). TFR is a homodimeric 190 kDa glycosylated transmembrane protein composed of two identical subunits which are linked by two disulfide bonds (*11*). The TFR dimer has a butterfly-like shape. Each of the two subunits possesses a transmembrane endodomain and an ectodomain of ∼700 amino acids directed toward the biological fluid. This ectodomain contains the transferrin-binding sites (*11*, *12*). The crystal structure of an ectodomain subunit was recently established (*12*). Each of these subunits can interact with one iron-loaded protein (*12*, *13*). In neutral media, TFR does not seem to possess any affinity for the

* To whom correspondence should be addressed. Telephone: 33144276807. Fax: 33144276814. E-mail: chahine@paris7.jussieu.fr.

[1] Abbreviations: ST, human serum transferrin; TFR, serum transferrin receptor 1; apo-ST, iron-free transferrin; holo-ST, iron-saturated transferrin; T-jump, temperature jump; CHAPS, 3-[(3-cholamidopropyl)dimethylammonio]-1-propanesulfonate; c_0, TFR analytical concentration; c_1, transferrin analytical concentration; TFe_2, holotransferrin in neutral media in an unknown state; $(TFe_2TFR)''$, one site of the thermodynamic form of the holotransferrin−receptor 1 adduct in an unknown state; $(TFR)'$, one interaction site of a form of receptor 1 in an unknown state; $(TFe_2TFR)'$, one site of an intermediate of the holotransferrin−receptor adduct; TFRa and $(TFRa)'$, one interaction site of receptor 1 in mildly acidic media in unknown states of protonation and charge, respectively; T, apotransferrin; $(T\text{-}TFRa)''$, one site of the thermodynamic apotransferrin receptor 1 adduct in mildly acidic media in an unknown state.

10.1021/bi030142g CCC: $27.50 © 2004 American Chemical Society
Published on Web 01/24/2004

iron-free protein (apo-ST) and the apparent affinity constants for binding of TFR to the iron-saturated ST and C-site-only iron-loaded ST equal $\sim 5 \times 10^8$ M^{-1} (*9*).

Many of the literature results deal with measurements of the affinity of the receptor for holo-ST (*9*, *14*−*17*). In vitro, it was recently shown by fluorescence correlation spectroscopy that the interaction of TFR with holo-ST is bimolecular under pseudo-first-order conditions (*17*). The kinetics of transfer of iron from the holo-ST−TFR adduct to pyrophosphate were also analyzed and showed that TFR facilitates the release of iron from transferrin (*18*). It was also shown that the holo-ST binding capacities of TFR, when fixed to a polystyrene surface, depend on the pH, bivalent ions, and temperature (*16*). The mechanism of interaction of TFR and transferrin is still not very well known.

In this work, by the use of the methods of chemical relaxation and the Joule effect temperature-jump (T-jump) technique (*19*−*23*), we analyze the kinetics and thermodynamics of the interactions of holotransferrin and apotransferrin with TFR in neutral and mildly acidic media, respectively. This allows us to propose a mechanism for the interaction between the two proteins in the pH range of 5−9.

EXPERIMENTAL PROCEDURES

More than 98% pure human serum apotransferrin (Sigma) was further purified by published procedures; its purity was checked spectrophotometrically, and by urea and SDS−polyacrylamide gel electrophoresis (*9*). KCl (Merck Suprapur), NaOH, HCl (Merck Titrisol), EDTA (Merck Titriplex), $FeCl_3$, trisodium citrate, acetic acid (96%), sodium acetate (Merck), sodium bicarbonate, glycerol, urea, SDS, boric acid, 3-[(3-cholamidopropyl)dimethylammonio]-1-propanesulfonate (CHAPS) (Ultra grade), dithiothreitol (DTT), phenylmethanesulfonyl fluoride (PMSF), Triton TX-100, ethanolamine, glycine (electrophoresis reagent), sodium azide (Sigma), lissamine rhodamine sulfonyl chloride (Acros), ammonium sulfate, nitrilotriacetic acid [$N(AcH)_3$], bromophenol blue, Brilliant blue, Hepes (Aldrich), acrylamide, APS, TEMED (Boehringer Mannheim), dibasic potassium phosphate trihydrate (Calbiochem), NaCl (molecular biology grade from Merck), and Sephadex G50 (Pharmacia) were used without further purification. Desferrioxamine was a gift from Novartis. Water and glassware were prepared as described previously (*24*).

Stock Solutions. All stock solutions were prepared in previously boiled doubly distilled water, sterilized afterward at 120 °C, and used fresh. Phosphate-buffered saline (PBS) was prepared from dibasic potassium phosphate trihydrate and NaCl. The Hepes concentration in neutral buffers ranged from 5 to 50 mM, and the acetate concentrations in acidic buffer were 50 mM. Final pHs were adjusted to 7− 9 with microquantities of concentrated HCl or NaOH. Transferrin concentrations (c_1) were spectrophotometrically checked and solutions diluted further to the required final concentrations in the buffers. $FeNAc_3$ solutions were prepared as previously described (*24*). All final ionic strengths in the Hepes or acetate buffers were adjusted to 0.2 M with KCl.

Metal-Loaded Transferrins. The iron-saturated serum transferrin was prepared as described elsewhere (*4*). The iron load was always checked by polyacrylamide−urea gel electrophoresis (*25*).

TFR Purification. TFR was extracted from human placenta and purified on an Affigel 15 (Bio-Rad) column doped with holotransferrin according to the published procedures and by following the protocol of Turkewicz *et al*. (*10*) as modified by Bali *et al*. (*18*). Purity was checked by gradient SDS−PAGE (*10*, *18*). TFR was obtained pure and used complete without cleaving the endodomain. Protein concentrations were determined spectrophotometrically and with a Bio-Rad protein assay. The final TFR concentration varied from 4 to 6 mg per placenta. TFR solutions were dialyzed four times against the final buffer. Final TFR concentrations (c_0) were achieved by dilution. Human placenta-screened HIV-free and hepatitis C-free were provided by the maternity hospital of the town of Ivry, France.

TFR Labeling with Rhodamine. The transferrin labeling method of Wahl and Azizi (*26*) was used to mark TFR in interaction with holotransferrin during TFR purification. Just before the acidification of the Affigel column with TFR fixed on holotransferrin (*10*, *18*), the gel was abundantly washed with a 1 M bicarbonate solution at pH 9. Then a solution of 35 μM lissamine rhodamine sulfonyl chloride in a 4:1 dioxane/dimethylformamide mixture was eluted through the column. After ~1 h, the column was washed with 50 mM ammonium chloride and abundantly washed with PBS. The receptor afterward was eluted and its purity checked by gradient SDS−PAGE as reported elsewhere (*10*, *18*). The fluorescence emission spectra of the labeled TFR with an excitation λ_{ex} of 573 nm and an emission λ_{em} of 593 nm (rhodamine fluorophore) and with a λ_{ex} of 280 nm and a λ_{em} of 310 nm (*9*) along with a protein assay showed a probable labeling of six rhodamines per receptor. This method will be further extended to a semispecific labeling of TFR, and the results will be reported later.

Spectrophotometric Measurements. Absorption measurements were performed at 37 ± 0.1 °C on a Cary 500 spectrophotometer equipped with a thermostated cell carrier. Differential absorption was accomplished by using two double-compartment cuvettes. In both cuvettes, one compartment was filled with a TFR solution while the other was filled with an ST solution. The solutions in the sample cell were mixed before measurements, while the two solutions in the reference cell remained separated. Fluorimetric measurements were performed at 37 ± 0.1 °C on an Aminco-Bowman series 2 luminescence spectrometer equipped with a thermostated cell carrier. The excitation wavelength was set to 280 or 573 nm for the native or rhodamine-labeled TFR, respectively. The spectra used for the static determination of equilibrium constants were recorded at the final thermodynamic state (1−3 h after mixing).

Fast Kinetic Measurements. Fast kinetic measurements were performed on a modified Joule effect Messanlagen und Studien absorption and fluorescence emission T-jump spectrophotometer. The apparatus was equipped with a 200 W Hg−Xe light source, a Jarrel Ash monochromator, and a thermostated cell holder kept at 25 ± 1 °C. Two capacitors were used for our experiments (0.01 and 0.05 μF). The 0.01 μF condenser was loaded with 30 kV, leading under our experimental conditions to a temperature jump of ~5 K with a heating time of ~1 μs, whereas the 0.05 μF capacitor was loaded with 23 kV, leading to a temperature jump of ~12 K with a heating time of ~5 μs (*23*). The signal was acquired on a personal computer equipped with a Synchronie fast

analog-to-digital converter and on a 150 MHz LeCroy 9430 digital oscilloscope. The signals were gathered at least 10 times and normalized.

Experimental Settings. In the TFR concentration (c_0) range (0.2−0.5 μM), the use of the CHAPS detergent is required to solubilize the receptor (*10*, *27*). For a c_0 of >0.1 μM, in the absence of CHAPS we encountered protein aggregation and surface adhesion problems which considerably perturbed the experimental approach. Therefore, unless specified otherwise, all reported experiments were performed in the presence of 10 mM CHAPS. Spectrophotometric detection was used in all thermodynamic and kinetic runs. Indeed, apo-ST, holo-ST, and TFR present characteristic absorption and fluorescence emission spectra for an excitation wavelength (λ_{ex} = 280 nm) and an emission wavelength (λ_{em} > 300 nm) (*9*). We also used for most of our T-jump experiments in neutral media the TFR species labeled with six rhodamine moieties outside of its area of interaction with holo-ST. In this case, the excitation wavelength (λ_{ex}) was set at 573 nm for a maximum in emission (λ_{em}) at 593 nm.

Data Analysis. The data were investigated by either linear or nonlinear least-squares analysis. The uncertainties on the slopes and intercepts of the linear regressions are given as the standard deviations ($\pm\sigma$). All the observed kinetics were pure mono- or multiexponential. They were analyzed as reported elsewhere and dealt with as relaxation modes (*19*−*24*). All experimental conditions were set to allow the use of the methods and techniques of chemical relaxation (*21*). Furthermore, TFR is composed of two identical subunits containing one interaction site each with ST (*12*). Therefore, our analysis deals with the concentration of interaction sites ($2c_0$) and not with TFR concentration (c_0). The proton titrations of ST and holo-ST were performed in the early 1960s (*28*). However, the sites of interactions of both ST and TFR are, to the best of our knowledge, still undetermined, and their state of charge and protonation are unknown. Therefore, the charge of the protein species is not indicated, and the subscripts used for H are only relative values.

RESULTS

Two experimental approaches were adopted. In the first, we analyzed the thermodynamics and kinetics of the interaction of holo-ST with TFR in neutral media, and in the second, we dealt with those of apo-ST with TFR in mildly acidic media.

Interaction of Holo-ST with TFR in Neutral Media. At a fixed pH value and in the final equilibrated state, the variations in the emission spectra observed when holo-ST or monoferric C-site iron-loaded ST is added to a solution of TFR allow the determination of the apparent dissociation constant for one interaction site of TFR K_{obs}, as done previously for eq 1 at pH 7.4 (*9*).

$$TFe_2 + TFR \rightleftharpoons \text{unknown} \rightleftharpoons (TFe_2TFR)'' \qquad (1)$$

where $K_{obs} = [TFe_2][TFR]/[(TFe_2TFR)'']$, where TFe_2 is holo-ST, TFR is in an unknown state of conformation and protonation, and $(TFe_2TFR)''$ is the two-protein adduct in an unknown state.

This experiment performed at different fixed pH values shows a linear relationship between K_{obs} and $[H^+]$. This implies the probable involvement of one or several proton transfers in eq 1 (*7*).

Four possibilities can be envisaged to interpret these observations. In the first, protons are lost from TFR and from the holo-ST−TFR adduct with the same pK_a on protonation sites independent of the protein−protein interaction. In this case, K_{obs} would be independent of pH (*30*). Since K_{obs} depends on $[H^+]$, this first possibility is discarded. In the second case, protons can be lost from the holo-ST-TFR adduct after its formation (eqs 2 and 3).

$$TFR + TFe_2 \rightleftharpoons (TFe_2TFR)''H_n \qquad (2)$$

$$(TFe_2TFR)'' + nH^+ \rightleftharpoons (TFe_2TFR)''H_n \qquad (3)$$

where $K'_a = [(TFe_2TFR)''][H^+]^n/[(TFe_2TFR)''H_n]$ and $K' = [TFR][TFe_2]/[(TFe_2TFR)''H_n]$. $(TFe_2TFR)''$ is the final equilibrated species of the protein−protein adduct.

In the third case, holo-ST needs to be in the nonprotonated form to interact with TFR (eqs 4 and 5).

$$TFe_2 + mH^+ \rightleftharpoons (TFe_2)' \qquad (4)$$

$$TFR + (TFe_2)' \rightleftharpoons (TFe_2TFR)'' \qquad (5)$$

where $K'_{1a} = [TFe_2][H^+]^m/[(TFe_2)']$ and $K'_1 = [TFR'][(TFe_2)']/[(TFe_2TFR)'']$. $(TFe_2)'$ is the unprotonated species of holo-ST in an unknown state.

In the fourth case, TFR needs to lose *m* protons to interact with holo-ST.

$$(TFR)' + mH^+ \rightleftharpoons TFR \qquad (6)$$

$$(TFR)' + TFe_2 \rightleftharpoons (TFe_2TFR)'' \qquad (7)$$

where $K_{1a} = [(TFR)'][H^+]^m/[TFR]$. $(TFR)'$ is the nonprotonated receptor. In the case of eqs 2 and 3, K_{obs} can be expressed as eq 8 (Appendix) (*7*).

$$1/K_{obs} = K'_a/(K'[H^+]^n) + 1/K' \qquad (8)$$

In the case of eqs 4−7, K_{obs} can be expressed as eq 9 (Appendix) (*7*, *30*).

$$K_{obs} = K'_1 + K'_1[H^+]^m/(K_a) \qquad (9)$$

in which K_a can be K_{1a} and/or K'_{1a}.

Two linear least-squares regressions of the data against eqs 8 and 9 were attempted. The better line is obtained with eq 9 (Figure 1a,b). From the intercept and slope of the best line, a K'_1 of 2.3 ± 0.3 nM and a K_a of 10.0 ± 1.5 nM are determined (Figure 1a).

A fifth possibility can also be envisaged for the TFR−holo-ST interaction where protons may be lost from both proteins before protein adduct formation (eqs 4, 6, and 10).

$$(TFR)' + (TFe_2)' \rightleftharpoons (TFe_2TFR)'' \qquad (10)$$

This fifth possibility implies the loss of at least two protons, one from each of the two proteins forming the TFR−holo-ST adduct. However, the fact that a single proton dissociation is involved in this adduct formation excludes this hypothesis.

To select the most probable mechanism for Fe_2T−TFR formation, a choice is to be made between case 3 (eqs 4 and

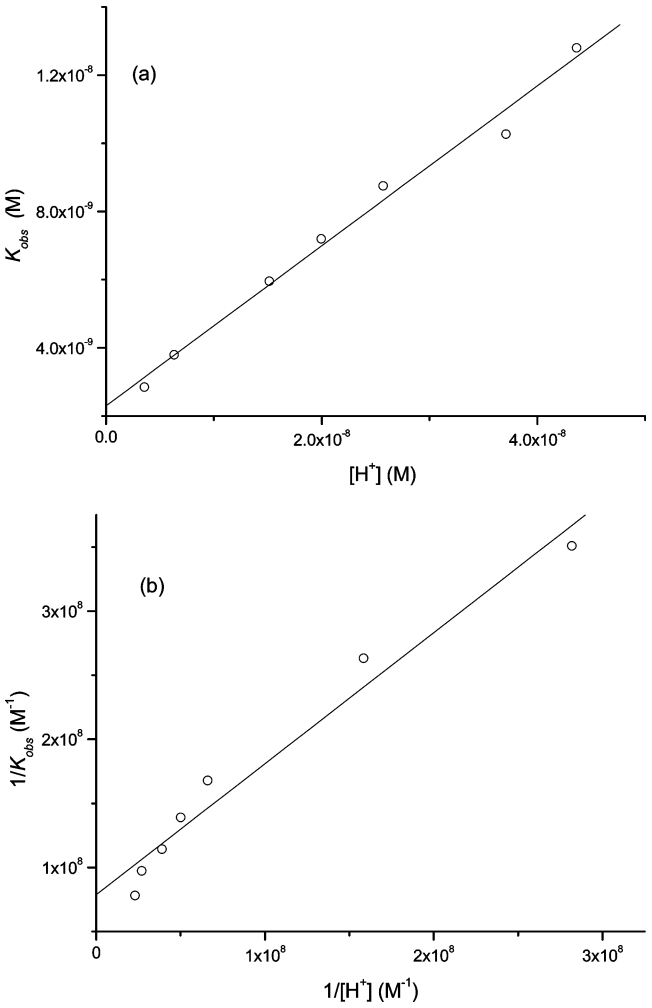

FIGURE 1: (a) Plot of K_{obs} vs $[H^+]$. Intercept = 2.3 ± 0.3 nM; slope = 0.23 ± 0.01, and r = 0.99383. (b) Plot of $1/K_{obs}$ vs $1/[H^+]$. Intercept = (7.9 ± 2) × 10^7 M^{-1}; slope = 1 ± 0.2, and r = 0.98317. Values reported at 37 ± 0.1 °C, μ = 0.2, and in the presence of 10 mM CHAPS.

5) and case 4 (eqs 6 and 7). Under our experimental conditions (pH 7.2−8.6) and in the presence of CHAPS, a spectrophotometric proton titration of holotransferrin showed a probable proton dissociation occurring below pH 7.2. This, of course, does not imply the absence of any proton dissociation between pH 7 and 9 (*28*, *29*), but simply shows that if this protonation occurs, it is not observed by spectrophotometric detection. On the other hand, near neutrality the fluorescence emission spectra of TFR vary with pH. If we assume that this variation depicts TFR proton dissociation (eq 6) with an m of 1, we can write eq 11 (Appendix) (*23*, *24*).

$$\Delta f/\Delta F = 1/2c_0 + [H^+]/(2K_{1a}c_0) \qquad (11)$$

where $\Delta F = F_0 - F$ and $\Delta f = f_{(TFR)'} - f_{TFR}$, in which F_0 is the fluorescence emission of the TFR species, F is the fluorescence emission, and $f_{(TFR)'}$ and f_{TFR} are the experimental proportionality constants which relate the fluorescence emission to the (TFR)′ and TFR concentrations, respectively. They were measured at pH <7 and >9.2, respectively.

A very good linear least-squares regression of $\Delta f/\Delta F$ against $[H^+]$ is obtained (Figure 2). From the slope of the regression line, a K_{1a} of 9.0 ± 1.0 nM is determined. This

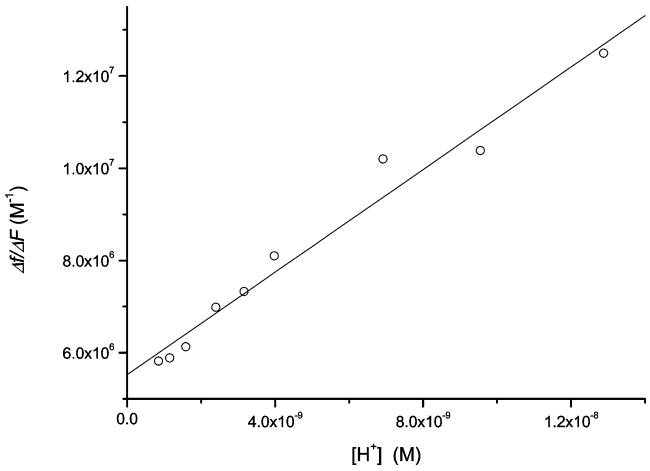

FIGURE 2: Plot of $\Delta f/\Delta F$ vs $[H^+]$ at 37 ± 0.1 °C, μ = 0.2, c_0 = 0.1 μM, and in the presence of 10 mM CHAPS. Intercept = (5.5 ± 0.5) × 10^6 M^{-1}; slope = (5.5 ± 0.5) × 10^{14} M^{-2}, and r = 0.98573.

value is, within the limits of uncertainty, identical to K_a. We shall, therefore, assume that the interaction of TFR and holo-ST obeys eqs 6 and 7.

Kinetics of the Interaction of Holo-ST with TFR. When a solution of TFR is submitted to a fast T-jump, a fast decrease in the fluorescence emission is detected. This process is not time-resolved by the Joule effect T-jump technique as it is not observed in the absence of CHAPS. Furthermore, no kinetic process is observed when a holo-ST solution in the presence or absence of CHAPS is submitted to the same T-jump. On the other hand, at least three kinetic processes are detected upon addition of holo-ST to a solution of TFR in neutral media. The first two processes are fast and detected by the T-jump technique, whereas the third is very slow and is detected by differential absorption variation with time (Figure 3). The two fast processes are observed after performing a T-jump on a solution of TFR immediately after addition of holo-ST. The first process occurs, as with TFR alone, as an extremely fast decrease in the fluorescence emission, whereas the second occurs in the range of 50−100 μs as an exponential increase in the fluorescence emission (Figure 3a). These two processes are observed with both native and rhodamine-labeled TFR. In this last case, the signal-to-noise ratio is high enough to allow signal analysis with ∼10 accumulations, whereas with the native protein, many more accumulations are required. Under similar conditions, with both the native and labeled proteins, the experimental reciprocal relaxation times $[(\tau_1)^{-1}]$ associated with the second kinetic process of Figure 3a are, within the limits of uncertainty, identical. This implies that the rhodamine labeling does not affect the kinetic analysis. The first process of Figure 3a is not time-resolved by the Joule effect T-jump technique. The experimental $(\tau_1)^{-1}$ values depend on TFR and holo-ST (c_1) concentrations. As for the third kinetic process, it seems to be independent of all our experimental parameters and occurs with a constant relaxation time (τ_2) of 3400 ± 600 s. Apart from the first ultrafast process of Figure 3a, all the other kinetic processes were also detected in the absence of CHAPS.

Figure 3a shows at least two kinetic processes occurring upon equilibrium perturbation by a fast T-jump performed on a solution containing TFR and holo-ST in neutral media.

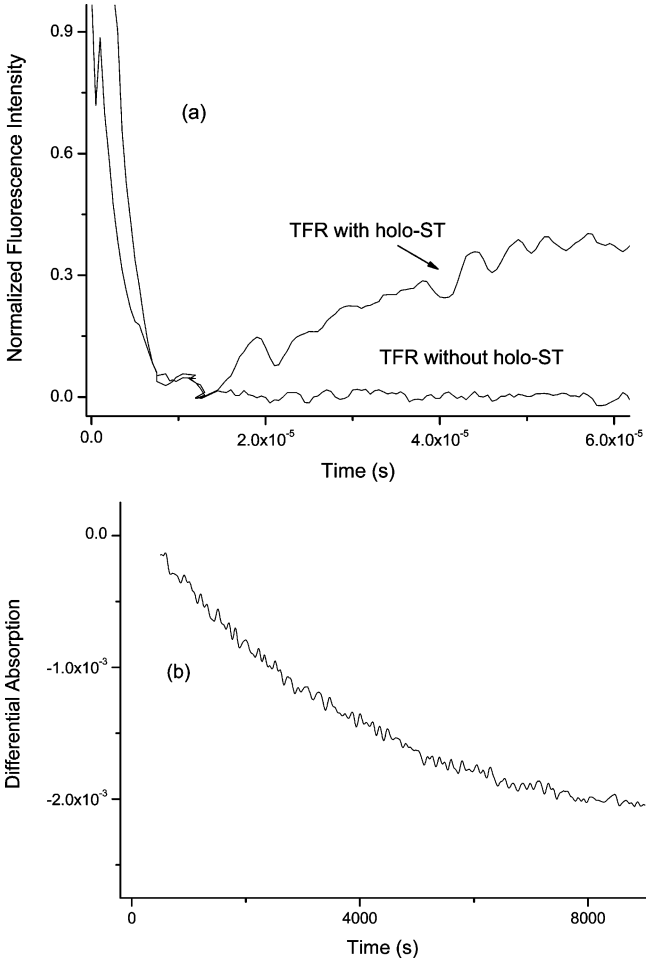

FIGURE 3: (a) Normalized variation of fluorescence emission with time when a solution of rhodamine-labeled TFR in the absence and presence of holo-ST is submitted to a fast T-jump with the following: $c_0 = 0.22\ \mu$M, $c_1 = 0.88\ \mu$M, and [CHAPS] = 10 mM at 37 ± 1 °C, $\mu = 0.2$, and pH 8.02. Reported for a λ_{ex} of 570 nm and a λ_{em} of >595 nm. (b) Differential absorption variation with time at 280 nm between unmixed (reference) and mixed solutions of TFR and holo-ST with the following: $c_0 = 0.11\ \mu$M, $c_1 = 0.66\ \mu$M, and [CHAPS] = 10 mM at 37 ± 0.1 °C, $\mu = 0.2$, and pH 8.02.

We cannot directly connect the first fast process with eq 6. Indeed, proton transfer reactions are usually diffusion-controlled (*31*, *32*). The second-order kinetic constants of diffusion-controlled proton transfers are on the order of 10^9−10^{11} M^{-1} s^{-1} (*31*, *32*). Therefore, under our experimental conditions at several fixed pH values (pH 7.2−8.6), the proton dissociation would occur in the range of 1−100 ms [$\sim 1/(10^{9-11} \times [H^+])$ s] (*20*, *21*). Thus, the first and second kinetic processes of Figure 3a are much too fast to be ascribed to eq 6. The first fast process is not observed in the absence of CHAPS. Therefore, this first time-unresolved process shall be discussed later (Discussion). The fact that for technical reasons we are not under the conditions of equilibrium 7 ($K_1' \ll c_0$ and c_1) excludes the possibility that equilibrium perturbation by the T-jump directly affects eq 7 (*20*). However, the dependence of experimental $(\tau_1)^{-1}$ on c_0 and c_1 led us in a first approximation to ascribe the second kinetic process of Figure 3a to a direct reaction between an interaction site of TFR and holo-ST which may constitute one step in eq 7 leading to the accumulation of kinetic intermediate $(TFe_2TFR)'$ (eq 12).

$$(TFR)' + TFe_2 \underset{k_{-1}}{\overset{k_1}{\rightleftharpoons}} (TFe_2TFR)' \qquad (12)$$

where $K_1 = k_{-1}/k_1 = [(TFR)'][TFe_2]/[(TFe_2TFR)']$.

Under our experimental conditions ($c_1 > 5c_0$), the reciprocal relaxation time associated with eq 12 is expressed as eq 13 (*20*, *21*).

$$(\tau_1)^{-1} \approx k_{-1} + k_1[TFe_2] \qquad (13)$$

If we assume that the process of Figure 3a occurs before proton dissociation (eq 6), eq 13 can be expressed as eq 14 (Appendix).

$$(\tau_1)^{-1} \approx k_{-1} + k_1[c_1 - 2c_0[H^+]/([H^+] + K_{1a})] \qquad (14)$$

A good linear least-squares regression of the experimental $(\tau_1)^{-1}$ against $c_1 - 2c_0[H^+]/([H^+] + K_{1a})$ is obtained (Figure 4). From the slope and intercept of the best line, a k_1 of (3.20 ± 0.20) × 10^{10} M^{-1} s^{-1}, a k_{-1} of (1.6 ± 0.2) × 10^4 s^{-1}, and a K_1 of 0.50 ± 0.07 μM are obtained.

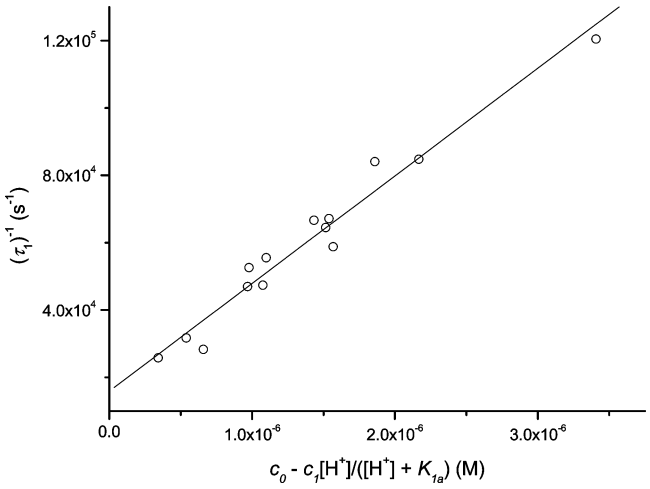

FIGURE 4: Plot of $(\tau_1)^{-1}$ vs $c_1 - 2c_0[H^+]/([H^+] + K_{1a})$ at [CHAPS] = 10 mM, $\mu = 0.2$, 37 ± 1 °C, and pH 7.2−8.4. Intercept = (1.6 ± 0.2) × 10^{-4} s^{-1}; slope = (3.2 ± 0.2) × 10^{10} M^{-1} s^{-1}, and r = 0.98451.

The third kinetic process of Figure 3b was also observed by other detection techniques and under different experimental conditions (*16*, *17*). Under the chemical relaxation conditions (*21*), it seems to be independent of all experimental parameters, with measured relaxation times (τ_2) of 3400 ± 600 s. Within the limits of uncertainty, this phenomenon can describe a first-order kinetic process (*4*−*7*, *20*, *21*), which can be attributed to a change in the conformation of TFe_2(TFR) (eqs 15 and 16) (*4*−*7*).

$$(TFe_2TFR)' \underset{k_{-2}}{\overset{k_2}{\rightleftharpoons}} (TFe_2TFR)'' \qquad (15)$$

$$(\tau_2)^{-1} = k_2 + k_{-2} \qquad (16)$$

and for one interaction site, $K_2 = k_{-2}/k_2 = [(TFe_2TFR)'']/[(TFe_2TFR)'] = K_1/K_1' = (4.6 \pm 1.0) \times 10^{-3}$.

At the end of this final process, the protein adduct attains its final equilibrated state.

Interaction of TFR with Apo-ST in Mildly Acidic Media. As in neutral media (*9*), at a constant pH value and at

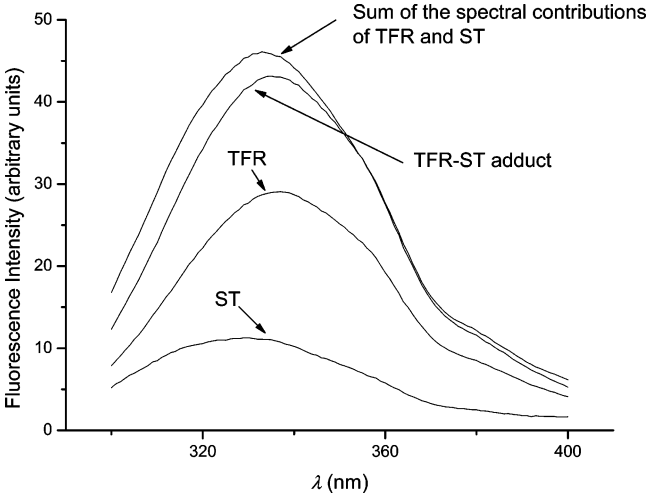

FIGURE 5: Fluorescence emission spectra of apo-ST, TFR, and TFR in the presence of 1 equiv of apo-ST. Values reported at 37 ± 0.1 °C, $\mu = 0.2$, pH 5.50, and [CHAPS] = 10 mM with the following: $c_0 = 42.1$ nM for an λ_{ex} of 280 nm and an λ_{em} of 337 nm.

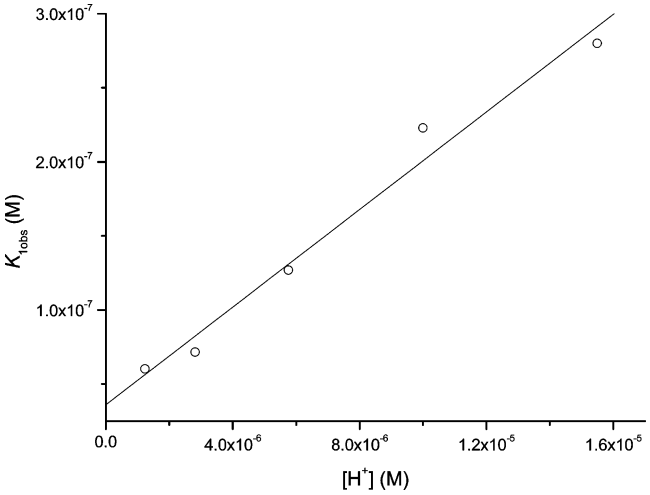

FIGURE 6: Plot of K_{1obs} vs [H$^+$] at 37 ± 0.1 °C and $\mu = 0.2$ in the presence of 10 mM CHAPS. Intercept = 36 ± 10 nM; slope = (1.6 ± 0.1) × 10^{-2}, and $r = 0.98956$.

thermodynamic equilibrium, the variation in the emission spectra observed when apo-ST is added to a solution of TFR (Figure 5) allows the measurement of the apparent dissociation constant (K_{1obs}) for one interaction site of TFR with apo-ST (eq 17).

$$\mathrm{T} + \mathrm{TFRa} \rightleftharpoons \text{unknown} \rightleftharpoons (\text{T-TFRa})'' \qquad (17)$$

where T stands for apo-ST, TFRa for the acidic form of TFR and T-TFRa for TFRa in interaction with aop-ST at pH 4.9−6.2 in an unknown state, and $K_{1obs} = [\mathrm{T}][\mathrm{TFRa}]/[(\text{T-TFRa})'']$.

As in neutral media with holotransferrin, this experiment performed at different fixed pH values shows a linear relationship between K_{1obs} and [H$^+$] (Figure 6). This implies the probable involvement of one or several proton transfers in eq 18 and allows us to write eqs 18−20 (*7*, *30*).

$$(\mathrm{TFRa})' + l\mathrm{H}^+ \rightleftharpoons \mathrm{TFRa} \qquad (18)$$

$$(\mathrm{TFRa})' + \mathrm{T} \rightleftharpoons (\text{T-TFRa})'' \qquad (19)$$

$$K_{1obs} = [\mathrm{H}^+]^l K_3'/K_{2a} + K_3' \qquad (20)$$

where (TFRa)′ is an intermediate, $K_3' = [(\mathrm{TFRa})'][\mathrm{T}]/[\mathrm{T}(\mathrm{TFRa})'']$, $K_{2a} = [(\mathrm{TFRa})'][\mathrm{H}^+]^l/[\mathrm{TFRa}]$, and l is the number of protons involved.

The best linear least-squares regression of K_{1obs} against $[\mathrm{H}^+]^l$ is obtained for an l of 1 (Figure 6). A K_3' of 36 ± 10 nM and a K_{2a} of 2.3 ± 0.3 μM are determined from the intercept and slope of the best regression line.

Kinetics of the Interaction between Apo-ST and TFR. In mildly acidic media (pH between 4.9 and 6.2), when a solution containing TFR is submitted to fast T-jump after addition of apo-ST, an ultrafast decrease (<1 μs) in the fluorescence intensity is detected. This process is also observed with TFR in the absence of apo-ST and is not detected in the absence of CHAPS. Furthermore, when apo-ST is added to a solution of TFR, a second kinetic process is also detected. It appears as an exponential decrease in the fluorescence intensity with time, which occurs in the range of 1000 s (Figure 7). TFR does not interact with apo-ST in

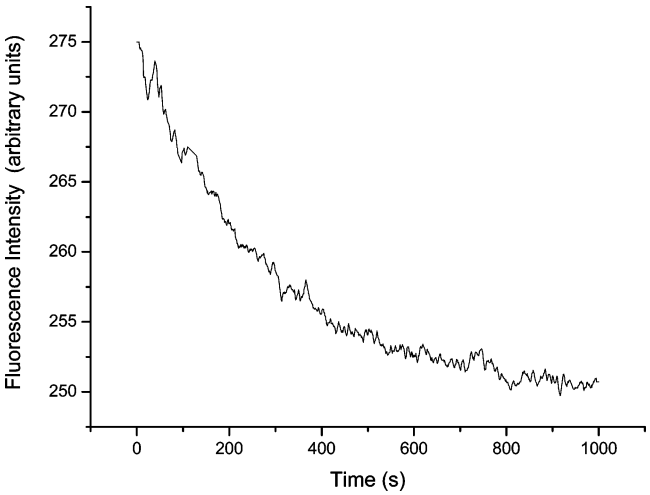

FIGURE 7: Fluorescence emission variation with time when a solution of TFR is mixed with a solution of apo-ST in mildly acidic media with the following: $c_0 = 42$ nM, $c_1 = 93$ nM, and [CHAPS] = 10 mM at 37 ± 0.1 °C, $\mu = 0.2$, and pH 6.14 for a λ_{ex} of 280 nm and a λ_{em} of 337 nm.

neutral media. We shall, therefore, assume that apo-ST interacts with TFR in a state different from that encountered in neutral media (TFRa).

The ultrafast kinetic process observed after performing a fast T-jump on TFR occurs in the presence or absence of apo-ST and is not observed in the absence of CHAPS. As in neutral media, this process will be dealt with in the Discussion. The experimental reciprocal relaxation times $[(\tau_3)^{-1}]$ associated with the slow kinetic process of Figure 7 do not directly depend on protein concentrations. This, therefore, excludes a bimolecular process related to the interaction between the two proteins (*20*−*24*). Furthermore, if we assume that this slow process follows an undetected fast interaction between apo-ST and TFR, the experimental reciprocal relaxation time $(\tau_3)^{-1}$ should, as in neutral media, be independent of the concentrations of the species present in the medium (*4*−*7*, *20*, *21*). Since this is not the case, two other possibilities can be envisaged here. In the first, the process of Figure 7 can be related to a rate-limiting modification in the conformation of apo-ST (eq 21) to adapt for the interaction with the acidic form of the receptor (eq

22). In the second case, the acidic form of TFR will undergo a rate-limiting change in conformation to interact with apo-ST (eqs 23 and 24).

$$T \underset{k'_{-3}}{\overset{k'_3}{\rightleftharpoons}} T' \text{ (rate-limiting)} \quad (21)$$

$$T' + (TFRa)' \rightleftharpoons (T'\text{-}TFRa)' \quad (22)$$

where $K'_4 = [(TFRa)'][T']/[(T'\text{-}TFRa)']$ and $K''_3 = [T]/[T']$.

$$(TFRa)' \underset{k_{-3}}{\overset{k_3}{\rightleftharpoons}} (TFRa)'' \text{ (rate-limiting)} \quad (23)$$

$$(TFRa)'' + T \rightleftharpoons (T\text{-}TFRa)'' \quad (24)$$

where $K_4 = [(TFRa)''][T]/[(T\text{-}TFRa)'']$ and $K_3 = [(TFRa)']/[(TFRa)'']$.

The reciprocal relaxation time equation associated with eqs 21 and 23, when either is rate-limiting, can be expressed as eqs 25 (when $c_0 > c_1$) and 26 (when $c_1 > c_0$), respectively (Appendix).

$$(\tau_3)^{-1} \approx k'_{-3}K'_4/[(TFRa)'] + k'_3/\{1 + K'_4/[(TFRa)']\} \quad (25)$$

$$(\tau_3)^{-1} \approx k_{-3}K_4/[T] + k_3[K_{2a}/(K_{2a} + [H^+])](1 + K_4/[T]) \quad (26)$$

Two series of kinetic runs were performed. In the first (designed to analyze eq 25), the pH and c_1 were fixed whereas c_0 was variable and greater than $4c_1$. In the second series (designed to analyze eq 26), the pH and c_0 were fixed and c_1 was varied and greater than $4c_0$.

The experimental reciprocal relaxation times $[(\tau_3)^{-1}]$ related to the first series of experiments are independent of c_0. This is not compatible with eq 25 and, thus, rejects eqs 21 and 22.

In the case of eqs 23 and 24, [T] can easily be determined as the positive solution of a quadratic equation (eq 27):

$$K_{2a}[T]^2 - [(c_1 - 2c_0)K_{2a} + K_{2a}K'_3 + K'_3[H^+]][T] - 2K'_3c_0(K_{2a} + [H^+]) - (c_1 - 2c_0)(K_{2a}K'_3 + K'_3[H^+]) = 0 \quad (27)$$

Under the experimental conditions used for this analysis ([T] $> 2c_0$, K_4, and K_3), eq 26 can be expressed as eq 28.

$$(K_{2a} + [H^+])(\tau_3)^{-1} \approx k_{-3}K_4(K_{2a} + [H^+])/[T] + k_3K_{2a} \quad (28)$$

A very good linear least-squares regression of the data against eq 28 is obtained (Figure 8). From the slope, a $k_{-3}K_4$ of $(7.9 \pm 0.6) \times 10^{-10}$ s^{-1} is determined. The uncertainty on the intercept is much too high to allow the determination of k_3K_{2a}.

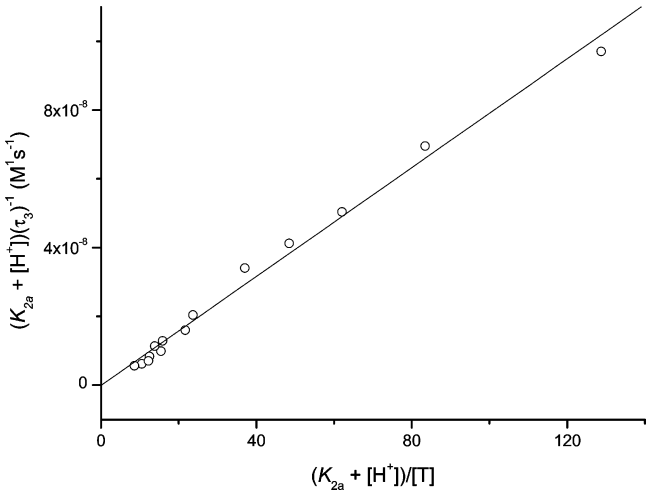

FIGURE 8: Plot of $(K_{2a} + [H^+])(\tau_3)^{-1}$ vs $(K_{2a} + [H^+])/[T]$. Intercept $= (-4 \pm 100) \times 10^{-11}$ M s^{-1}; slope $= (7.9 \pm 0.6) \times 10^{-10}$ s^{-1}, and $r = 0.99535$.

DISCUSSION

The apparent dissociation constants K_{obs} (eq 1) of the holo-ST−TFR species measured in the absence of detergent are very close to those measured in the presence of CHAPS (*9*). Therefore, CHAPS does not seem to influence the interaction between the two proteins. Nevertheless, CHAPS is a zwitterionic surfactant with a critical micelle concentration (CMC) of ~3 mM at $\mu = 0.2$ (*33*). This implies that at the concentrations used here (10 mM) it will form micelles (*33*). We used for our experiments only the complete TFR without cleaving the ectodomain. This whole receptor forms aggregates in a purely aqueous medium, whereas it is monomolecular in the presence of CHAPS (*34*). This can explain the solubility and surface adhesion problems encountered when our experiments are performed with TFR concentrations ($c_0 \geq 0.2$ μM). TFR is homodimeric with an endodomain anchored in the plasma membrane and an ectodomain directed toward the biological fluids (*12*, *34*). CHAPS micelles have an average aggregation number of 4−20 and can be considered small micelles compared to TFR (*33*). However, micelles can adapt their size and their shape or cooperate to solubilize large molecules such as proteins (*35*). CHAPS can, therefore, play here the role of an artificial membrane with the micelles solubilizing the transmembrane domain while the hydrophilic water-soluble ectodomain is still directed toward the aqueous medium (*34*). An aqueous micelle dissociates in two kinetic steps (*23*, *36*). The first occurs in <1 μs and corresponds to the dissociation of one monomer from the micelle. The interaction of the guest molecule with the micelle also occurs in the same time range (*36*). As for the second kinetic step, it occurs in the millisecond range and corresponds to the total dissociation of the micelle into its monomers (*23*, *36*). In the range of 25−50 °C, the CMC of CHAPS decreases with temperature (*37*). This implies that under our experimental conditions, the micellar equilibrium is perturbed by the T-jump from 25 to 37 °C. In addition, neither of the kinetic processes observed with TFR in the absence or presence of holo-ST in neutral media (Figure 3a) and in acidic media is observed in the absence of CHAPS, as they are not time-resolved by the Joule effect T-jump technique (<1 μs). We can, therefore, ascribe them to CHAPS micelle dissociation under the influence of the T-jump or the interaction of the proteins with CHAPS. This will not, however, affect the kinetic approach dealing with the second fast process of Figure 3a, which still occurs in the absence of CHAPS in the range of 50 μs. As for the whole dissociation of the micelle into its monomers, it is much too slow to affect this second kinetic process and much too fast to affect the slow processes of Figures 3b and 7 (*23*).

Table 1: Mechanism of Interaction of TFR with Holo- and Apotransferrin

equation	direct rate constant	reverse rate constant	equilibrium constant
$(TFR)' + H^+ \rightleftharpoons TFR$ (eq 6)			10.0 ± 1.5 nM
$(TFR)' + TFe_2 \rightleftharpoons (TFe_2TFR)'$ (eq 12)	$(3.20 \pm 0.20) \times 10^{10}$ M^{-1} s^{-1}	$(1.6 \pm 0.2) \times 10^4$ s^{-1}	0.50 ± 0.07 μM
$(TFe_2TFR)' \rightleftharpoons (TFe_2TFR)''$ (eq 15)			$(4.6 \pm 1.0) \times 10^{-3}$
$(TFR)' + TFe_2 \rightleftharpoons (TFe_2TFR)''$ (eq 7)[a]			2.3 ± 0.3 nM
$(TFRa)' + H^+ \rightleftharpoons TFRa$ (eq 18)			2.30 ± 0.30 μM
$(TFRa)' \rightleftharpoons (TFRa)''$ (eq 23)			
$(TFRa)'' + T \rightleftharpoons (T\text{-}TFRa)''$ (eq 24)			
$(TFRa)' + T \rightleftharpoons (T\text{-}TFRa)''$ (eq 19)[a]			36 ± 10 nM

[a] Equations 7 and 19 constitute the apparent interactions reactions between TFR and holo-ST or ST in neutral and mildly acidic media, respectively.

In Table 1, we summarize the mechanism of the interaction of ST and TFR in neutral and mildly basic media. We did not detect any kinetic process with holo-ST and apo-ST in the absence of TFR. TFR interacts with holo-ST and does not interact with apo-ST in neutral media, whereas it interacts with apo-ST in mildly acidic media. This interaction with apo-ST was reported in cell lines (*38*). Moreover, a change in the conformation of TFR upon acidification was also reported (*39*). This led us to envisage the existence of at least two different species of TFR, the neutral species which does not interact with apo-ST and the acidic species which interacts with apo-ST. In neutral physiological media, holo-ST is recognized by TFR with which it forms the $(TFe_2)_2$−TFR adduct responsible for transport of iron from the cell surface to the cytosol by endocytosis (*8*). In vitro, this molecular recognition takes place through eqs 12 and 15. The first step in the molecular interaction between TFR and holo-ST (eq 12) leads to the formation of an intermediate protein−protein adduct. This step (Figure 3a) is fast and occurs in the range of 50 μs, which is in agreement with the fact that molecular interactions involving proteins can be extremely fast (*40*, *41*). The affinity of TFR for holo-ST at the end of this fast process of Figure 3a equals 1.5×10^6 M^{-1} (eq 12, Table 1). Molecular interactions are normally the results of noncovalent bonds such as van der Waals, hydrogen, electrostatic, hydrophobic, and other weak to very weak bonds (*42*, *43*). The additivity principle can sometimes explain affinity values as high as K_1^{-1} (*43*). Further, TFR contains a highly conserved Arg-Gly-Asp sequence in the C-site region which is thought to bind to holo-ST (*44*). If this triad binds to a spatially complementary sequence in holo-ST, it will also contribute to the stability of the kinetic intermediate produced by eq 12. This kinetic protein adduct undergoes a slow change in its conformation (Figure 3b, eq 15, and Table 1) during which it achieves its thermodynamic form. The affinity constant involved in the whole process of interaction between TFR and holo-ST $(K_1')^{-1}$ (eq 7, Table 1) equals 4.35×10^8 M^{-1}. This implies that the slow change in the conformation of Figure 3b (eq 15, Table 1) brings to the final thermodynamic species a structural stabilization factor of ~290. This final change in conformation plays, therefore, a key role in stabilizing the TFR−holo-ST adduct.

With holo-ST in the absence of TFR, we did not observe by the T-jump technique any fast kinetic process which would have been associated with a fast change in the conformation in neutral media. Indeed, iron uptake and release by ST are under the control of the transition in the conformation from open to closed or from closed to open. In neutral media, this conformation change is slow and lasts more than 1 h (*4*). Consequently, we assumed that the first step of the interaction of TFR with holo-ST does not involve any change in the conformation of holo-ST. The holotransferrin closed structure is, thus, probably adapted to the recognition by a part of the ectodomain of TFR (eq 12). The structures of both the ectodomain of TFR and ST are known. However, that of the protein adduct is still unknown (*45*), and attempts to model the binding sites and surfaces of interaction of both proteins have, to the best of our knowledge, not yet been successful (*45*). This may be due to the fact that this interaction occurs by two steps, the second of which is a change in the conformation of the protein adduct. Therefore, in its thermodynamic state, the conformation of the protein adduct is not equivalent to what may be expected from the conformations of each protein when taken separately, as in the case of a simple docking between two complementary structures (*45*).

The apparent dissociation constant of the protein adduct is dependent on pH, as the adduct is formed with a TFR having lost a proton probably from each of the binding sites (eqs 6, 12, and 15 and Table 1). This proton loss ($pK_{1a} = 8$) is indispensable for the interaction between TFR and holo-ST, as the protonated TFR species does not react with holo-ST. Only eqs 6, 12, and 15 can explain our experimental data, which implies that this proton loss is a prerequisite for the interaction between the two proteins in neutral media. TFR does not interact with apo-ST. However, this interaction occurs in mildly acidic media with probably a TFR species (TFRa) different from that encountered in neutral media (eq 19). Here also a loss of a proton from the TFRa receptor species is involved (eq 18). This implies that the interaction of apo-ST with the receptor is controlled by the pH. Indeed, apo-ST interacts with only TFRa in the unprotonated form. This species should exist at only pH >4.5 ($pK_{2a} = 5.64$; eq 18, Table 1). During the receptor-mediated TFR−holo-ST iron delivery process, the protein adduct is transposed from the neutral bloodstream medium to the mildly acidic medium (pH ~5.5) of the final endosome in which iron is lost. TFR is then kept in an interaction with apo-ST, and the adduct is recycled back to the cell surface where apo-ST loses its affinity for TFR (*8*). In mildly acidic media (pH 4.9−6.2), the interaction between apo-ST and TFR is preceded by a slow change in the conformation of TFR which controls the final molecular interaction (eqs 23 and 24 and Table 1). Since iron is lost from the holo-ST−TFR adduct in the acidic endosome (*8*), it would have been interesting to analyze the interaction between holo-ST and TRFa. However, under our experimental conditions (pH <6), iron is lost within a few seconds from the N-site of holo-ST (*6*). This iron loss is faster than the rate-limiting step in the interaction of TFRa

with apotransferrin (eq 23, Table 1). Under these circumstances, it would be practically impossible for us to measure the kinetics of the interaction of holo-ST and TFR in mildly acidic media. The overall affinity of TFRa for apo-ST in acidic media is ~1 order of magnitude lower than that measured for TFR with holo-ST in neutral media [$(K'_3)^{-1} = 2.8 \times 10^7\ M^{-1}$; eq 19, Table 1]. In these acidic media and in contrast to neutral media, the interaction of apo-ST with TFRa is rate-controlled by an indispensable change in the conformation of TFRa prior to any molecular interaction (eqs 23 and 24 and Table 1). This slow change in conformation along with the affinity of TFRa for apo-ST allows the recycling of the TFRa−apo-ST adduct back to the plasma membrane. Upon endosome recycling to the surface of the cell in contact with the neutral medium, the lack of affinity of TFR for apo-ST (*8*, *9*) permits a new transferrin cycle. How and why this lack of affinity occurs is another matter.

CONCLUSION

In this article, we propose a mechanism for the interaction of transferrin with its receptor in the neutral media of biological fluids and in the mildly acidic media of the endosome. We suggest the existence of at least two different TFR species, the neutral species and the acidic species. The interaction of the neutral species of TFR with holo-ST is the starting step of the system of iron delivery by receptor-mediated endocytosis. As for the interaction of the acidic receptor with apotransferrin in the mildly acidic medium of the endosome, it permits the recycling of the protein adduct to the outer membrane at the cell surface where it dissociates, allowing another iron delivery cycle. We showed that the interaction of holotransferrin with the receptor is practically instantaneous and occurs with a medium-strength affinity constant. The structure of the adduct that is formed is consolidated by a slow conformation change which increases the affinity by more than 2 orders of magnitude. In mildly acidic media, a slow change in the conformation of the acidic species of the TFR, along with the overall affinity of this acidic species for apo-ST, permits the recycling of the protein−protein adduct back to the plasma membrane. Transposing directly these findings to natural media may, of course, be overoptimistic because they are based on results obtained in vitro in cell-free assays and in the presence of CHAPS micelles.

APPENDIX

Equation 8 is derived from the mathematical expressions of K', K'_a, and mass conservation at the final equilibrated state (eqs 29 and 30).

$$2c_0 = [\mathrm{TFR}] + [(\mathrm{TFe_2TFR})''\mathrm{H}_n] + [(\mathrm{TFe_2TFR})''] \quad (29)$$

$$c_1 = [\mathrm{TFe_2}] + [(\mathrm{TFe_2TFR})''\mathrm{H}_n] + [(\mathrm{TFe_2TFR})''] \quad (30)$$

Equation 9 is derived from the mathematical expressions of K_a', K'_1, and mass conservation at a final equilibrated state when the proton loss occurs from holo-ST (eqs 31 and 32) or TFR (eqs 32 and 34)

$$2c_0 = [\mathrm{TFR}] + [(\mathrm{TFe_2TFR})''] \quad (31)$$

$$c_1 = [\mathrm{TFe_2}] + [(\mathrm{TFe_2})'] + [(\mathrm{TFe_2TFR})''] \quad (32)$$

$$2c_0 = [\mathrm{TFR}] + [(\mathrm{TFR})'] + [(\mathrm{TFe_2TFR})''] \quad (33)$$

$$c_1 = [\mathrm{TFe_2}] + [(\mathrm{TFe_2TFR})''] \quad (34)$$

Equation 11 is derived from the expression of fluorescence intensities (eqs 35 and 36), the mathematical expression of K_{1a}, and mass conservation (eq 37).

$$F = f_{(\mathrm{TFR})}[\mathrm{TFR}] + f_{(\mathrm{TFR})'}[(\mathrm{TFR})'] \quad (35)$$

$$F_0 = f_{(\mathrm{TFR})}2c_0 \quad (36)$$

$$2c_0 = [\mathrm{TFR}] + [(\mathrm{TFR})'] \quad (37)$$

The rate equation associated with equilibrium 23 when rate-limiting can be expressed as eq 38.

$$-\mathrm{d}\Delta[(\mathrm{T\text{-}TFRa})'']/\mathrm{d}t = k_{-3}\Delta[(\mathrm{TFRa})''] - k_3\Delta[(\mathrm{TFRa})'] \quad (38)$$

The conservation of mass allows to write eqs 39 and 40.

$$\Delta[\mathrm{TFRa}] + \Delta[(\mathrm{TFRa})'] + \Delta[(\mathrm{TFRa})''] + \Delta[(\mathrm{T\text{-}TFRa})''] = 0 \quad (39)$$

$$\Delta[(\mathrm{T\text{-}TFRa})''] + \Delta[\mathrm{T}] = 0 \quad (40)$$

Equations 18 and 24 can be considered in a constant state of equilibrium during eq 23. We can, therefore, write eqs 41 and 42 for a constant pH value.

$$\Delta[(\mathrm{T\text{-}TFRa})''] = [(\mathrm{TFRa})'']\Delta[\mathrm{T}]/K_4 + [\mathrm{T}]\Delta[(\mathrm{TFRa})'']/K_4 \quad (41)$$

$$\Delta[\mathrm{TFRa}] = [\mathrm{H}^+]\Delta[(\mathrm{TFRa})']/K_{2a} \quad (42)$$

Equation 26 is determined from eqs 38−42 by substitution methods (*20*, *21*). Equation 25 is derived in a manner similar to that for eq 26. Equation 27 is derived from the mathematical expressions of K_4, K_{2a}, and the conservation of mass at the final equilibrated state (eqs 43 and 44).

$$2c_0 = [\mathrm{TFRa}] + [(\mathrm{TFRa})'] + [(\mathrm{TFRa})''] + [(\mathrm{T\text{-}TFRa})''] \quad (43)$$

$$c_1 = [(\mathrm{T\text{-}TFRa})''] + [\mathrm{T}] \quad (44)$$

REFERENCES

1. Aisen, P., Enns, C., and Wessling-Resnick, M. (2001) *Int. Biochem. Cell Biol. 10*, 940−959.
2. Moore, S. A., Anderson, B. F., Groom, C. R., Haridas, M., and Baker, E. N. (1997) *J. Mol. Biol. 274*, 222−236.
3. Zuccola, H. J. (1992) The crystal structure of monoferric human serum transferrin, Ph.D. Thesis, Georgia Institute of Technology, Atlanta, GA.
4. Pakdaman, R., Bou Abdallah, F., and El Hage Chahine, J. M. (1999) *J. Mol. Biol. 293*, 1273−1284.
5. Bou Abdallah, F., and El Hage Chahine, J. M. (1999) *Eur. J. Biochem. 263*, 912−920.
6. El Hage Chahine, J. M., and Pakdaman, R. (1995) *Eur. J. Biochem. 230*, 1102−1110.
7. Bou Abdallah, F., and El Hage Chahine, J. M. (2000) *J. Mol. Biol. 303*, 255−266.
8. Dautry-Varsat, A., Ciechanover, A., and Lodish, H. F. (1982) *Proc. Natl. Acad. Sci. U.S.A. 80*, 2258−2262.
9. Hémadi, M., Kahn, P. H., Miquel, G., and El Hage Chahine, J. M. (2003) *Biochemistry 42*, 3120−3130.

10. Turkewitz, A. P., Amatruda, J. F., Borhani, D., Harrison, S. C., and Schwartz, A. L. (1988) *J. Biol. Chem. 263*, 8318−8325.
11. Enns, C. A., and Sussman, H. H. (1981) *J. Biol. Chem. 256*, 9820−9823.
12. Lawrence, C. M., Ray, S., Babyonyshev, M., Galluster, R., Brhani, B. W., and Harrison, S. C. (1999) *Science 286*, 779−782.
13. West, A. P., Jr., Giannetti, A. M., Herr, A. B., Bennett, M. J., Nangiana, J. S., Pierce, J. R., Weiner, L. P., Snow, P. M., and Bjorkman, P. J. (2001) *J. Mol. Biol. 313*, 385−397.
14. Bali, P. K., and Aisen, P. (1992) *Biochemistry 31*, 3963−3967.
15. Fuchs, H., and Gessner, R. (2002) *Biochim. Biophys. Acta 1570*, 19−26.
16. Orberger, G., Fuchs, H., Geyer, R., Gessner, R., Kottgen, E., and Tauber, R. (2001) *Arch. Biochem. Biophys. 2386*, 79−88.
17. Schüler, J., Frank, J., Trier, U., Schäfer-Korting, M., and Saenger, W. (1999) *Biochemistry 38*, 8402−8408.
18. Bali, P. K., Zak, O., and Aisen, P. (1991) *Biochemistry 30*, 324−328.
19. Eigen, M., and DeMaeyer, L. (1963) Relaxation methods, in *Techniques of Organic Chemistry: Investigation of Rates and Mechanism of Reactions, Part II* (Friess, S. L., Lewis, E. S., and Weissberger, A., Eds.) Vol. 8, pp 895−1029, Wiley-Interscience, New York.
20. Bernasconi, C. F. (1976) *Relaxation Kinetics*, Academic Press, New York.
21. Brouillard, R. (1980) *J. Chem. Soc., Faraday Trans. 1 76*, 583−587.
22. Winkler-Oswatitsch, R., and Eigen, M. (1979) *Angew. Chem., Int. Ed. 18*, 20−49.
23. El Hage Chahine, J. M. (1990) *J. Chem. Soc., Perkin Trans. 2*, 1045−1050.
24. El Hage Chahine, J. M., and Fain, D. (1993) *J. Chem. Soc., Dalton Trans.*, 3137−3143.
25. Makey, D. G., and Seal, U. S. (1976) *Biochim. Biophys. Acta 453*, 250−256.
26. Wahl, P., and Azizi, F. (1997) *Biochim. Biophys. Acta 1327*, 69−74.
27. Schüler, J., Franck, J., Saenger, W., and Georgalis, Y. (1999) *Biophys. J. 77*, 1117−1125.
28. Hazen, E. E., Jr. (1962) A Titration Study of Transferrin, Ph.D. Thesis, Harvard University, Cambridge, MA.
29. Chasteen, N. D., and Williams, J. (1981) *Biochem. J. 193*, 717−727.
30. Bellounis, L., Pakdaman, R., and El Hage Chahine, J. M. (1996) *J. Phys. Org. Chem. 9*, 111−118.
31. Eigen, M., and DeMaeyer, L. (1955) *Z. Electrochem. 59*, 986−993.
32. Huang, H., Nishikawa, S., and Dong, S. (1999) *J. Phys. Chem. 103*, 8799−8802.
33. Le Maire, M., Champeil, P., and Moller, J. (2000) *Biochim. Biophys. Acta 1508*, 86−111.
34. Fuchs, H., Gessner, R., Tauber, R., and Ghosh, R. (1995) *Biochemistry 34*, 6196−6207.
35. Zdunek, J., Martinez, G. V., Schleucher, J., Lycksell, P. O., Yin, Y., Nilsson, S., Shen, Y., Olivecrona, G., and Wijmenga, S. (2003) *Biochemistry 42*, 1872−1889.
36. Aniansson, E. A. G., Wall, S. N., Almgren, M., Hoffmann, H., Klelmann, I., Ulbricht, W., Zana, R., Lang, J., and Tondre, C. (1976) *J. Phys. Chem. 80*, 905−922.
37. Partearroyo, M. A., Goni, F. M., Katime, I., and Alonso, A. (1988) *Biochem. Int. 16*, 259−265.
38. Klausner, R. D., Ashwell, G., van Renswoude, J., Harford, J. B., and Bridges, K. B. (1983) *Proc. Natl. Acad. Sci. U.S.A. 80*, 2263−2266.
39. Turkewitz, A. P., Schwartz, A. L., and Harrison, S. C. (1988) *J. Biol. Chem. 263*, 16309−16315.
40. Koren, R., and Hammes, G. G. (1976) *Biochemistry 15*, 1165−1171.
41. Deng, H., Zhadin, N., and Callender, R. (2001) *Biochemistry 40*, 3767−3773.
42. Israelachvili, J. (1994) *Intermolecular and Surface Forces*, Academic Press, London.
43. Kuntz, I. D., Chen, K., Sharp, K. A., and Kollman, P. A. (1999) *Proc. Natl. Acad. Sci. U.S.A. 96*, 9997−10002.
44. Dubljevic, V., Sali, A., and Goding, J. W. (1999) *Biochem. J. 341*, 11−14.
45. Yajima, H., Sakajiri, T., Kikuchi, T., Morita, M., and Ishii, T. (2000) *J. Protein Chem. 19*, 215−223.

BI030142G